JOURNAL OF MATERIALS SCIENCE 35 (2000) 5793–5807

Influence of whisker toughening and microstructure on the wear behavior of Si_3N_4- and Al_2O_3-matrix composites reinforced with SiC

C. P. DOĞAN, J. A. HAWK
U.S. Department of Energy, Albany Research Center, Albany, OR 97321-2198, USA
E-mail: dogan@alrc.doe.gov

A comparative study of the influence of randomly-oriented SiC whiskers on the abrasive wear behavior of several commercially-produced Si_3N_4- and Al_2O_3-based ceramics suggested that the residual stress states present within the materials can be important in predicting their wear resistance. The addition of SiC whiskers to the Si_3N_4 matrix created residual tensile stresses at the whisker-matrix interfaces which led to enhanced bulk fracture toughness, but which degraded the fracture toughness at the microstructural level, and thus the abrasive wear resistance, by promoting easier whisker debonding and removal by the abrasive particles. The addition of SiC whiskers to an alumina matrix, on the other hand, led to the creation of residual compressive stresses at whisker-matrix interfaces, producing a locally tougher interface that was more able to withstand the rigors of the abrasive wear environment. These results indicate that in brittle materials, improved bulk mechanical properties do not always translate directly to improved performance in a tribological environment.

1. Introduction

Ceramic-reinforced ceramic composites represent one of the more promising developments to date in the effort to produce tough, yet mechanically reliable, ceramic materials for advanced structural applications, and particularly for applications at elevated temperatures in severe environments. Over the course of the last decade, much research has gone into the understanding of precisely how the addition of reinforcement phases can influence the strength and toughness of the bulk ceramic material. For whisker-reinforced ceramic materials enhanced toughness can occur through any one, or several, of the following mechanisms: whisker pullout, crack bridging, and/or crack deflection [1–7]. In many cases, large scale toughening requires that (i.) the whisker-matrix interface be relatively weak to facilitate whisker debonding, and (ii.) toughening mechanisms be activated over some distance behind the tip of the propagating crack. As a result, while the long-crack toughness of the bulk material can be enhanced by the presence of the whisker reinforcement, the short-crack toughness may remain unchanged, or even be degraded, by the presence of these whiskers. Studies of how whisker reinforcement influences the tribological properties of ceramic materials are largely missing, although several studies have addressed the relative performance of whisker-reinforced ceramic matrix composites in sliding and abrasive wear environments [8–17]. However, one point is clear: the assumption that enhanced mechanical properties translate directly to enhanced wear resistance in whisker-reinforced ceramic composites can be an incorrect one.

A material's response to a wear environment is not purely an intrinsic one, but is rather a reaction to a complicated combination of stresses imposed by an external system that is defined by such variables as contact geometry, speed, load, temperature, lubrication and environment. Because of the complexity and variability of the stresses generated by such systems, a generic model that can reliably predict how ceramic materials will react in tribological environments continues to elude materials and design engineers. Nonetheless there is a desire, as well as a need, to rank prospective tribological materials based on intrinsic material properties. For the abrasive wear of brittle materials, mathematical models [18, 19] generally assume that subsurface lateral fracture is responsible for most material removal, leading to the prediction that volume wear will be inversely proportional to both the material's hardness and fracture toughness. Unfortunately, a number of studies on a wide variety of ceramic materials have indicated that conventionally-measured hardness and fracture toughness are often not good predictors of a ceramic's wear resistance [8, 9, 20]. This model, and others, fail to adequately describe the abrasive wear behavior of most advanced ceramic materials in at least one important way: they assume that bulk hardness and fracture toughness measurements are sufficient to describe the deformation and fracture characteristics of the test material in an abrasive wear environment. In

particular, it has been noted that in ceramic materials which exhibit increasing fracture toughness with increasing crack length, such as alumina, silicon nitride, zirconia, and many ceramic-reinforced composites, the measured bulk fracture toughness may not describe the fracture toughness of the ceramic at the microstructural scale where abrasive wear mechanisms are active [21–23]. In addition, many of the testing procedures commonly used to determine mechanical properties, such as fracture toughness, employ carefully controlled semi-equilibrium environments, which may not provide data relevant to the wear environment, where the forces imposed on the material can be both transient and variable [24]. Clearly then, there is a need for a better understanding of how these macrostructurally tough materials perform in environments where toughness on a microstructural scale is also an important factor. With that goal in mind, this study examines how microstructure and the presence of randomly-oriented SiC whiskers can influence the abrasive wear behavior of several commercially-produced silicon nitride- and alumina-based ceramic materials.

2. Experimental procedure

Three commercially-available, SiC-whisker reinforced composite materials were selected for this study, along with three chemically-similar, but unreinforced, matrix materials for comparison. All six materials were designed by their manufacturer to be "wear resistant." The first pair of silicon nitride-based materials were processed in an identical manner, except for the addition of 15 volume percent SiC whiskers to the composite material. This series had a predominantly crystalline grain boundary phase, and so was designated Si_3N_4-C and Si_3N_4-C + SiC_w for the monolith and composite, respectively. The second series of silicon nitride-based ceramics, Si_3N_4-G and Si_3N_4-G + SiC_w, were processed somewhat differently than the first in order to produce a glassy grain boundary phase; however, the composite material also contained 15 volume percent SiC whiskers. For the alumina-based materials, the composite, $Al_2O_3 + SiC_w$, consisted of 34 volume percent SiC whiskers in a high-purity alumina matrix. Because no similarly-processed monolithic alumina was available, a 99.8%Al_2O_3 of relatively high hardness was selected for comparison with the composite.

Microstructural characterization of these materials was performed primarily by transmission electron microscopy (TEM), in combination with chemical analysis by X-ray Energy Dispersive Spectroscopy (XEDS). In addition, X-ray diffraction (utilizing Cu K_α radiation) was employed to determine the primary matrix phase of the silicon nitride ceramics. Analysis of the materials' microstructural response to the various abrasive wear tests was by scanning electron microscopy (SEM) in secondary electron imaging mode. Sample preparation for TEM analysis followed traditional ceramographic techniques, including ion milling to electron transparency. Sample preparation for SEM analysis was limited to ultrasonic removal of the wear debris from the wear surfaces, followed by coating with a Au-Pd alloy to reduce charging in the microscope.

Hardness and fracture toughness were measured for each material on surfaces mechanically polished to a 1 μm diamond finish. Vickers hardness was determined under a load of 1 kg, with a dwell time of 15 seconds. Ten separate hardness measurements were taken for each material, with the results averaged. Fracture toughness was measured utilizing the indentation technique described by Anstis *et al.* [25] with an identing load of 10 kg. A minimum of five fracture toughness measurements were made for each material and the results averaged.

Material response to two-body abrasive wear was measured utilizing a pin abrasion test designed at the Albany Research Center to simulate abrasion that occurs during crushing and grinding operations. This test is described in detail elsewhere [26], and will not be discussed here; however, it is important to recognize that during this test, the sample was continually exposed to fresh abrasive. The ceramics and ceramic composites of this study were identically tested against four different abrasive cloths: 150-grit Al_2O_3 (nominal abrasive particle size of 100 μm; average hardness of 18.6 GPa); and 400-, 240- and 150-grit SiC (with nominal abrasive particle sizes of 37, 58, and 100 μm, respectively, and with an average hardness of 23.1 GPa). In each of these tests the pin sample, 6.35 mm in diameter, was abraded under an applied load of 66.7 N (corresponding to an average applied pressure of 2.11 MPa), for a distance of 16 m. Abrasive wear was expressed as the specific wear rate, W_s, calculated according to the equation [27]:

$$W_s = \frac{\Delta m}{\rho L F_N} \tag{1}$$

where Δm was the mass loss of the test specimen under the test conditions described; ρ was the density of the test sample measured using Archimedes principle; L was the sliding distance; and F_N was the normal force applied to the pin through the chuck assembly. Table I contains a summary of the results of the pin-on-drum tests, including the number of tests run on each sample for each abrasive type, the average mass loss, the standard deviation, and the coefficient of variation. The standard deviations listed in Table I were calculated using the "small sample size" statistical analysis recommended for abrasive wear testing in the appendix of ASTM G65 [28]. This method of calculating the standard deviation utilized the range of measured mass loss values for each sample set, and thus typically yielded a higher value for the standard deviation than did root mean square deviation analyses. However, because of the smaller sample size, the results were more representative of the actual error. Inspection of Table I indicates that the values for the coefficient of variation for these tests ranged from a low of 0.7% to a high of 6.2%. The average coefficient of variation was 3.2%. Thus differences in test results greater than ~6% were attributable to real differences in the wear behavior of the materials.

To better understand the microstructural response of the ceramics to individual events occurring in the abrasive wear environment, a series of single-pass scratch

TABLE I Data from the abrasive wear tests of the ceramics and ceramic composites, including standard deviations (S.D.) and coefficients of variation (C.O.V)

Material	Abrasive Type, Size	#Tests	Average Mass Loss (g)	S.D. (g)	C.O.V. (%)
Si_3N_4-C	Al_2O_3, 100 μm	6	2.97	0.16	5.3
	SiC, 100 μm	9	31.84	1.21	3.8
	SiC, 58 μm	6	23.33	0.47	2.0
	SiC, 37 μm	3	8.63	0.24	2.7
Si_3N_4-C + SiC_w	Al_2O_3, 100 μm	6	3.53	0.12	3.4
	SiC, 100 μm	7	33.05	1.66	5.0
	SiC, 58 μm	6	23.58	0.43	1.8
	SiC, 37 μm	3	6.40	0.18	2.8
Si_3N_4-G	Al_2O_3, 100 μm	6	5.73	0.36	6.2
	SiC, 100 μm	6	43.05	1.22	2.8
	SiC, 58 μm	6	30.62	0.55	1.8
	SiC, 37 μm	3	10.30	0.35	3.4
Si_3N_4-G + SiC_w	Al_2O_3, 100 μm	4	6.55	0.21	3.3
	SiC, 100 μm	6	49.35	0.79	1.6
	SiC, 58 μm	1	33.40	—*	—*
	SiC, 37 μm	2	11.70	0.35	3.0
99.8% Al_2O_3	Al_2O_3, 100 μm	5	6.42	0.21	3.3
	SiC, 100 μm	6	36.22	0.36	1.0
	SiC, 58 μm	6	24.65	1.34	5.4
	SiC, 37 μm	6	8.67	0.36	4.1
Al_2O_3 + SiC_w	Al_2O_3, 100 μm	4	2.82	0.08	2.8
	SiC, 100 μm	6	18.58	0.13	0.7
	SiC, 58 μm	6	12.74	0.25	2.0
	SiC, 37 μm	6	3.47	0.19	5.5

Average C.O.V. = 3.2% ± 1.5%.
*Insufficient material available to conduct additional wear tests.

tests were performed on each material with a conical diamond indenter (tip radius equal to 20 μm), under normal loads of 150, 200, 250, and 300 grams, at a speed of 100 μm/min. The resulting scratches were examined using both optical microscopy and SEM.

3. Results

3.1. Microstructure

Micrographs illustrating the general microstructural features of the three composite materials, and the monolithic 99.8%Al_2O_3, can be found in Fig. 1, and an outline of the microstructural characteristics of all of the ceramics examined in this study can be found in Table II. All of the ceramics and ceramic composites tested are liquid-phase sintered materials in which the matrix grains are bonded by a continuous crystalline and/or amorphous grain boundary phase. The composition and nature of these grain boundary phases depend upon the additives and impurities introduced into the materials during processing, and the total thermal history of the ceramic. In the Si_3N_4-C ceramic, this grain boundary phase is primarily crystalline $Y_2Si_3N_4O_3$, with some β-$Y_2Si_2O_7$; however, a narrow, amorphous silicate phase is also observed at the homo- and heterophase boundaries, and is expected to be a continuous phase in these materials. Bend contours, suggesting residual strain, are visible at many of the heterophase boundaries, although the residual stress is not sufficient to cause microcracking at any of the grain boundaries observed. The Si_3N_4-C + SiC_w composite (Fig. 1a) is microstructurally identical except for the distribution of randomly oriented, intergranular SiC whiskers, which, with an average diameter of 1 μm and average aspect ratio of 10 : 1, are large relative to the matrix grains. Although not apparent at the magnification of the micrograph in Fig. 1a, a thin amorphous silicate phase also wets the $SiC_w - Si_3N_4$, $SiC_w - Y_2Si_3N_4O_3$, and $SiC - Y_2Si_2O_7$ boundaries.

The matrix microstructure of the second series of silicon nitride ceramics, Si_3N_4-G, consists of a distribution of Si_3N_4 grains which are larger than those in the C-series (average matrix grain size is 0.75 μm as compared to 0.4 μm in Si_3N_4-C), bonded by an amorphous yttrium aluminosilicate phase that is also believed to be continuous in these materials. This amorphous phase is observed at the homo- and heterophase interfaces (including the whisker-matrix interfaces) in both the

TABLE II Microstructural characteristics of the ceramics and ceramic composites

Material	Matrix Grain Size (μm)	Primary Matrix Phase	Primary Grain Boundary Phase(s)	SiC Reinforcement
Si_3N_4-C	0.4	β-Si_3N_4	Crystalline $Y_2Si_3N_4O_3$, β-$Y_2Si_2O_7$	—
Si_3N_4-C + SiC_w	0.4	β-Si_3N_4	Crystalline $Y_2Si_3N_4O_3$, β-$Y_2Si_2O_7$	Random, Intergranular
Si_3N_4-G	0.75	β-Si_3N_4	Amorphous Y, Al Silicate	—
Si_3N_4-G + SiC_w	0.75	β-Si_3N_4	Amorphous Y, Al Silicate	Random, Inter- & Intragranular
99.8% Al_2O_3	2.0	α-Al_2O_3	Crystalline Graphite, β-Al_2O_3	—
Al_2O_3 + SiC_w	4.0	α-Al_2O_3	Amorphous Mg, Al Silicate	Random, Inter- & Intragranular

monolithic and composite Si_3N_4-G ceramics. Bend contours suggestive of residual stress are also apparent in this series of silicon nitrides, although not as pronounced. The microstructure of the composite is similar to that of the monolith (Fig. 1b), except for the presence of randomly oriented SiC whiskers, which have an average diameter of 0.75 μm and a variable aspect ratio. In this case, the whiskers are located both intragranularly (i.e., either partially or entirely encapsulated within a Si_3N_4 grain) and intergranularly within the microstructure.

For the alumina-based ceramics, the microstructures vary quite a bit between the monolithic and composite materials. The 99.8%Al_2O_3 (Fig. 1c) contains graphite at most three- and four-grain junctions, which extends along many of the two-grain alumina-alumina boundaries. These microstructures have not been examined by high-resolution TEM, and so it is not clear whether or not the graphite is a continuous phase in this material. In addition to the graphite, elongated "whiskers" of a potassium-modified β-Al_2O_3 phase are also occasionally observed at the grain boundaries. Significant stresses are apparent at the α-Al_2O_3–β-Al_2O_3 interfaces; however because the population of such interfaces is relatively small within this material, the presence of this stress is unlikely to influence the

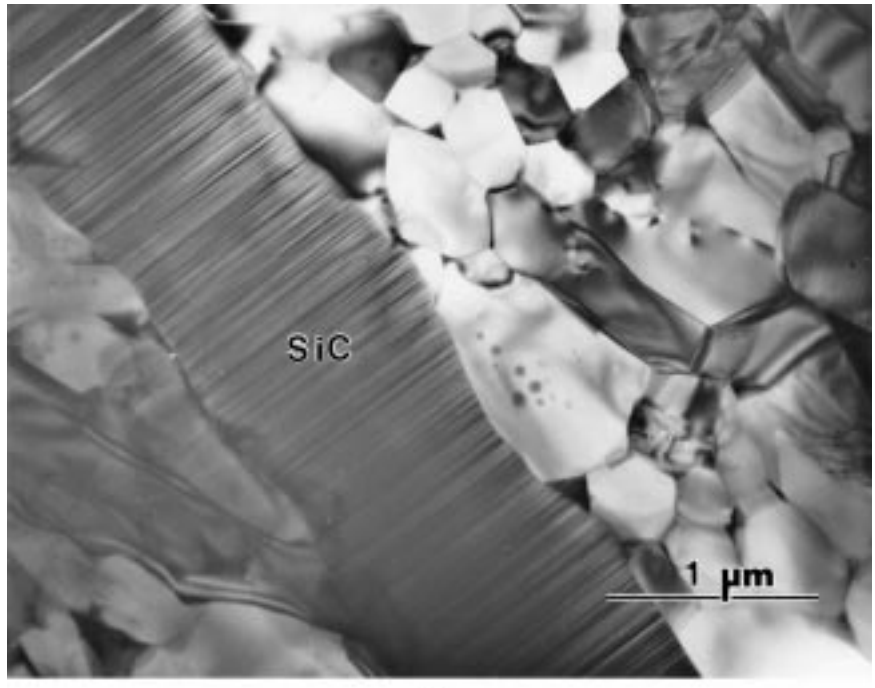

(a)

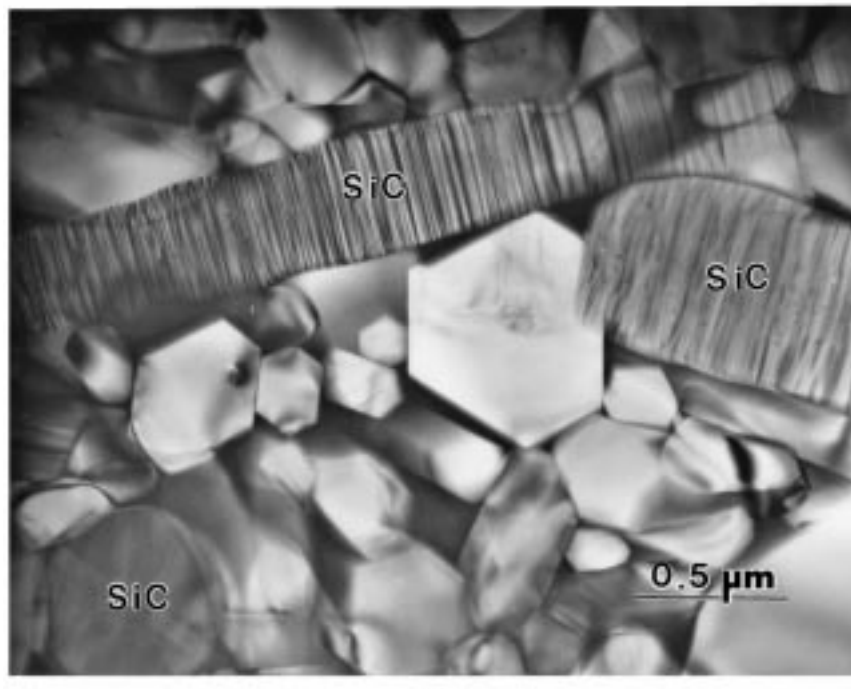

(b)

Figure 1 General microstructural features of (a) the Si_3N_4-C + SiC_w composite; (b) the Si_3N_4-G + SiC_w composite; (c) the 99.8%Al_2O_3 ("α" and "β" refer to α-Al_2O_3 and β-Al_2O_3, respectively); and (d) the Al_2O_3 + SiC_w composite ("Gr" refers to graphite). (*Continued*)

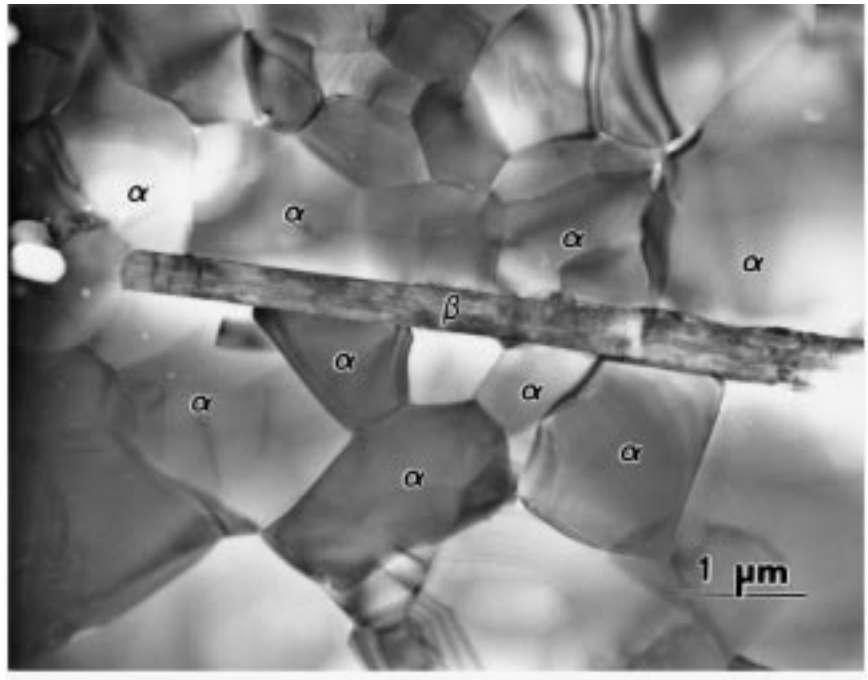

(c)

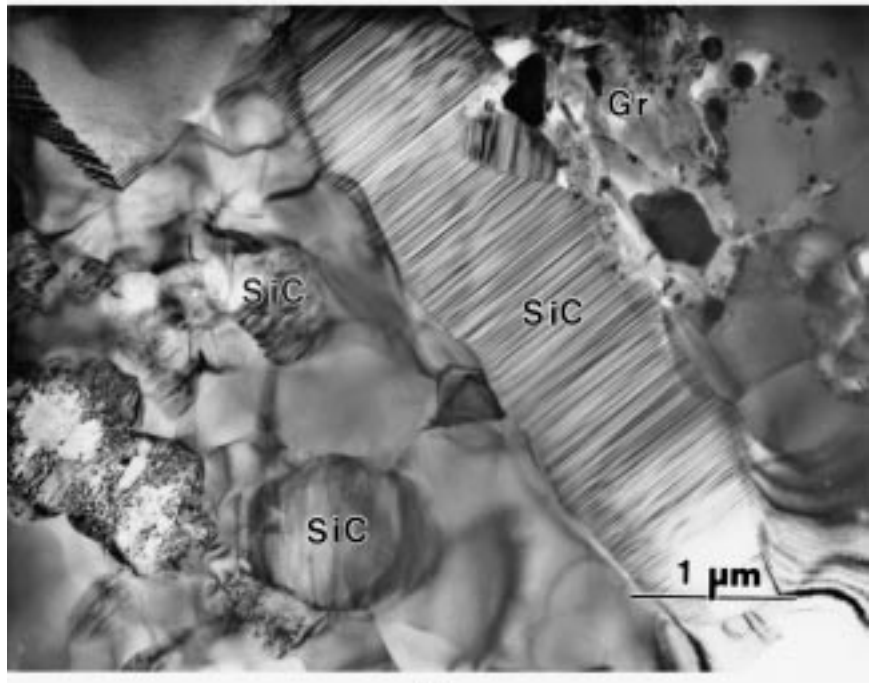

(d)

Figure 1 (*Continued*).

tribological properties of the bulk material. The alumina grain size in this material averages around 2 μm, although there are also pockets of much smaller, submicron, grains within the microstructure. In contrast, the alumina-based composite, $Al_2O_3 + SiC_w$, is a glass-bonded ceramic (Fig. 1d), containing approximately two volume percent of an amorphous magnesium aluminosilicate phase that is located at the three- and four-grain junctions and along most two-grain boundaries. This amorphous phase is also observed as a thin layer (<50 nm) at whisker-matrix interfaces. The SiC whiskers, with an average diameter of 0.75 μm and a variable aspect ratio, are distributed randomly throughout the alumina matrix and occur both inter- and intragranularly. Under dynamical imaging conditions, stress contours indicative of a residual tensile stress [29] are visible in the Al_2O_3 grains surrounding the intragranular whiskers. In amorphous pockets adjacent to the intergranular SiC whiskers, small crystals of graphite and an iron-nickel intermetallic are often observed (as in Fig. 1d). Alumina grain size within this composite averages around 4 μm.

3.2. Hardness and fracture toughness

Measured values for density, hardness and fracture toughness, along with reported values for Young's modulus (as provided by the manufacturers), are listed in

TABLE III Physical and mechanical properties of the ceramics and ceramic composites

Material	Density (g/cm^3)	Young's Modulus (GPa)$^+$	Hardness (GPa)*	Fracture Toughness (MPa$\sqrt{m}$)*
Si_3N_4-C	3.29	310	15.6 ($\pm$0.2)	5.4 ($\pm$0.3)
Si_3N_4-C + SiC_w	3.27	335	19.0 ($\pm$0.4)	6.4 ($\pm$0.3)
Si_3N_4-G	3.26	303	15.0 ($\pm$0.2)	5.5 ($\pm$0.3)
Si_3N_4-G + SiC_w	3.27	335	16.5 ($\pm$0.5)	5.4 ($\pm$0.3)
99.8% Al_2O_3	3.93	400	19.3 ($\pm$0.5)	3.4 ($\pm$0.5)
Al_2O_3 + SiC_w	3.64	395	23.8 ($\pm$1.1)	4.6 ($\pm$0.1)

$^+$Data provided by the respective manufacturers.
*Standard deviations for these values are in parentheses.

Table III for all of the ceramic materials examined in this study. The alumina-based materials, $Al_2O_3 + SiC_w$ and 99.8%Al_2O_3, have the highest hardness, with values of 23.8 and 19.3 GPa, respectively; whereas the unreinforced silicon nitrides, Si_3N_4-G and Si_3N_4-C, have the lowest hardness with values of 15.0 and 15.6 GPa, respectively. The addition of silicon carbide whiskers to the silicon nitride and alumina matrices results in an increase in the hardness of the composite in all cases. The variation in hardness measurements does not exceed $\pm$5% for any of the ceramics tested, although there is more variation in the measured hardness of the composites than in that of the monoliths, thanks to the presence of the relatively harder SiC whiskers.

Indentation fracture toughness measurements do not always provide the most accurate measure of the bulk fracture toughness of a ceramic, often resulting in values lower than those obtained by other measurement techniques [25]; however, the indentation technique is selected here because it is believed to provide a value more representative of the near surface regions of material exposed to an abrasive wear environment. And as expected, the measured values for fracture toughness obtained in this study are somewhat lower than those provided by the manufacturer for identical materials, or quoted in the literature for similar materials. Nonetheless, the toughness values measured in this study follow the same trend as those reported by the manufacturer. It is apparent from Table III that as a class of materials, the alumina-based ceramics are not as tough as the silicon nitride-based ceramics, and that the 99.8%Al_2O_3 has the lowest toughness of all of the materials tested in this study. The addition of SiC whiskers to Si_3N_4-C results in a 20% increase in toughness, making Si_3N_4-C + SiC_w the highest toughness material of this study, whereas the addition of SiC whiskers results in no real change in the toughness of Si_3N_4-G. The variation in toughness measurements is consistently less than 10% for all of the ceramics tested, except for the 99.8% alumina, where the variation is closer to 15%.

3.3. Abrasive wear behavior

The measured specific wear rates for all of the ceramics and ceramic composites tested against alumina and silicon carbide abrasives are listed in Table IV. The 100 μm alumina abrasive is clearly the least aggressive for all of the ceramics tested. Against the SiC abrasives, an increase in abrasive wear rate with increase in SiC abrasive particle size is observed for all of the ceramics and ceramic composites over the abrasive size range of 37 μm to 100 μm (Fig. 2). An interesting aspect of this data is the large increase (150–300%) in wear with increase in SiC abrasive particle size from 37 μm (400-grit) to 58 μm (240-grit). Such a large difference in wear rate over a relatively small change in abrasive particle size suggests a change in wear mechanisms [30], and in fact such a change is observed at the wear surfaces. Following wear against the 37 μm SiC abrasive, examination of the wear surfaces indicates that the response of these materials is primarily one of deformation, with only minimal fracture observed. Examination of the wear surfaces following the test against the 58 μm SiC, on the other hand, indicates that fracture has become a significant material response to the wear environment.

Under the various abrasive wear conditions of this study, monolithic Si_3N_4-C is consistently a better performer than is monolithic Si_3N_4-G, particularly against the "softer" alumina abrasive. Examination of the wear surfaces of these materials after abrasion against 100 μm alumina indicates that both materials are in the mild wear regime, where fracture toughness is predicted to dominate wear behavior [31]. Yet, there is no real difference in the measured fracture toughness of the two monolithic Si_3N_4's (Table III). A comparison of the top performing silicon nitride (Si_3N_4-C) with the 99.8% Al_2O_3, shows that the alumina, with the higher hardness but lower fracture toughness, possesses a lower wear rate for all SiC abrasive environments. Against the softer alumina abrasive, however, Si_3N_4-C has a 75% lower wear rate than the 99.8%Al_2O_3, no doubt because of its higher fracture toughness.

TABLE IV Specific wear rates for ceramics tested against various abrasives, with an applied load of 66.7 N and a sliding distance of 16 m

	Specific Wear Rate ($\times 10^{-3}$ mm^3/N-m)			
Material	100 μm Al_2O_3	100 μm SiC	58 μm SiC	37 μm SiC
Si_3N_4-C	0.85	9.07	6.61	2.46
Si_3N_4-C + SiC_w	1.01	9.47	6.76	1.83
Si_3N_4-G	1.65	12.39	8.81	2.93
Si_3N_4-G + SiC_w	1.88	14.14	9.57	3.35
99.8% Al_2O_3	1.53	8.64	5.88	2.07
Al_2O_3 + SiC_w	0.45	4.78	3.28	0.89

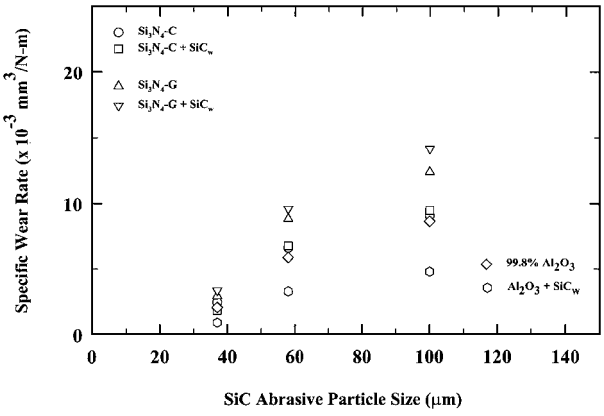

Figure 2 Plot of the specific wear rate versus SiC abrasive particle size for all materials examined in this study.

Perhaps the most interesting result of this study is the observation that the addition of 15 volume percent SiC whiskers to a silicon nitride matrix either does not affect the abrasive wear behavior of the bulk material, or degrades it slightly (Fig. 2). This trend occurs in spite of the fact that the addition of SiC whiskers increases the hardness of both Si_3N_4's and increases the fracture toughness of Si_3N_4-C. The only exception to this rule is in the Si_3N_4-C ceramics tested against 37 μm SiC, where the composite outperforms the monolith. In the alumina-based ceramics, on the other hand, the addition of SiC whiskers leads to a dramatic improvement in the abrasive wear resistance under all test conditions of this study. In fact, with its high hardness and respectable fracture toughness, $Al_2O_3 + SiC_w$ is by far the most wear resistant material examined in this study.

3.4. Microstructural response to the single scratch

When the conical diamond indenter scratches the surface of the silicon nitride and alumina ceramics of this study, the material responds by deformation and/or fracture. The specific mechanisms activated in this series of experiments of course depend upon the load applied to the diamond as well as the characteristics of the material. However in all cases, as the diamond moves across the surface, a plastic groove (the scratch) is formed. Heavily deformed material extruded from beneath the indenter is pushed to the sides and piles up at the edges of the scratch. Although often similar in appearance to the plastically deformed pile-ups which form at the sides of scratches in ductile materials, pile-ups in these more brittle ceramics are formed by the accumulation of material that is heavily microcracked along the grain boundaries and which has a high dislocation density within grains [32–34]. As a result, these highly stressed regions will often fracture, leaving fine-scale debris at either side of the scratch. Within the scratch, surface fracture frequently occurs at the trailing edge of the indenter and at the scratch periphery, where tensile stresses are highest. As the load is increased on the indenter, lateral cracks formed beneath the scratch extend to the surface, often times resulting in the removal of large chips of material. These subsurface lateral cracks can extend many times the scratch width to either side of the scratch, and represent a key source of material removal during the scratching of these ceramics.

Specific examples of the microstructural response to a single scratch test under a 200-gram load are illustrated in Fig. 3. In all cases, the silicon nitride based materials exhibit more plastic deformation, whereas the aluminas show more intra- and intergranular fracture, particularly within the wear groove. The Si_3N_4-G consistently exhibits a wider, deeper scratch, as well as more fracture in the pile-up region, than does Si_3N_4-C, although both Si_3N_4-based materials respond to the diamond indenter in approximately the same way. For all materials as the load is increased on the diamond indenter (up to 300 g), the level of damage within the scratch increases; however, the mode of damage does not change. The exception to this is the Si_3N_4-C monolith and the $Al_2O_3 + SiC_w$ composite, neither of which shows any evidence of fracture, and only minimal deformation, under a scratch load of 150 grams. Si_3N_4-C exhibits only minimal fracture at the scratch periphery under a load of 200 grams (Fig. 3a), in contrast to the Si_3N_4-C composite (Fig. 3b), which exhibits extensive fracture at the scratch periphery and cracking within the scratch trace under identical test conditions. In the alumina-based ceramics (Fig. 3c and d), the debris at the edges of the scratch on the 99.8% Al_2O_3 is of a larger scale than that at the periphery of the scratch in the $Al_2O_3 + SiC_w$ composite in spite of the fact that the average grain size of the monolith is approximately half that of the composite. Reflected light microscopy reveals far more subsurface fracture directly beneath the scratch trace in the 99.8%Al_2O_3 than in any of the other ceramics examined.

3.5. Microstructural response to abrasive wear

Whereas the scratch test involves a single interaction between an abrasive "particle" (the diamond indenter) and a surface, the pin-on-drum test involves the interaction of multiple abrasive particles of various shapes and orientations, and under variable loads, with a surface. As a result, the microstructural response to the abrasive environment can be much more difficult to interpret. Examples of several wear surfaces following abrasion against the 100 μm SiC (the most aggressive test of this study) are provided in Fig. 4. From these and other observations [35–37], it is apparent that one of the characteristic microstructural responses of a ceramic to an abrasive wear environment is the formation of a damage layer, or wear sheet, at the surface being abraded. Debris from individual abrasive-surface interactions, as well as from the fracture of abrasive particles, accumulates and is bonded together by the force and heat generated as the drum and sample surfaces move past one another. Some years ago, Hockey [38] observed part of this damage layer using TEM, and noted that the surface grains of a polycrystalline high alumina ceramic contain a high dislocation density. Similar observations have been made by the present authors in abraded ceramics containing between 85% and 99.997% alumina [19, 39]. Recently, Odén and Ericsson [40] also reported direct TEM observations of a deformation layer, some

1 to 2 μm thick, at the surface of a machined SiC-whisker reinforced alumina. A cross-sectional view of the wear sheet at the surface of a polycrystalline high-alumina ceramic (not the 99.8% Al_2O_3 of this study, although representative of it) abraded by 100 μm SiC is illustrated in Fig. 5a. A similar deformation layer is observed at the wear surface of the silicon nitride ceramics, as illustrated in the cross-sectional view of Si_3N_4-G in Fig. 5b. However, as is apparent in a comparison of Fig. 5a and b, the thickness of the wear sheet which develops depends upon the deformation and fracture characteristics of the matrix material, as well as on the bulk microstructure. For the materials of this study, the silicon nitride ceramics have a wear sheet that is approximately twice as thick as that which forms on the alumina ceramics; further, Si_3N_4-G with an amorphous boundary phase and larger matrix grain size, has a thicker wear sheet than does the Si_3N_4-C. The addition of SiC whiskers does not seem to influence the development of the wear sheet in either the oxide or the nitrides, although the presence of whiskers does appear to make the wear sheets more susceptible to fracture.

Superimposed on the wear sheet are the effects of the most recent individual abrasive particle-surface interactions. In the C-series of silicon nitride materials, the principal response to the SiC wear environment

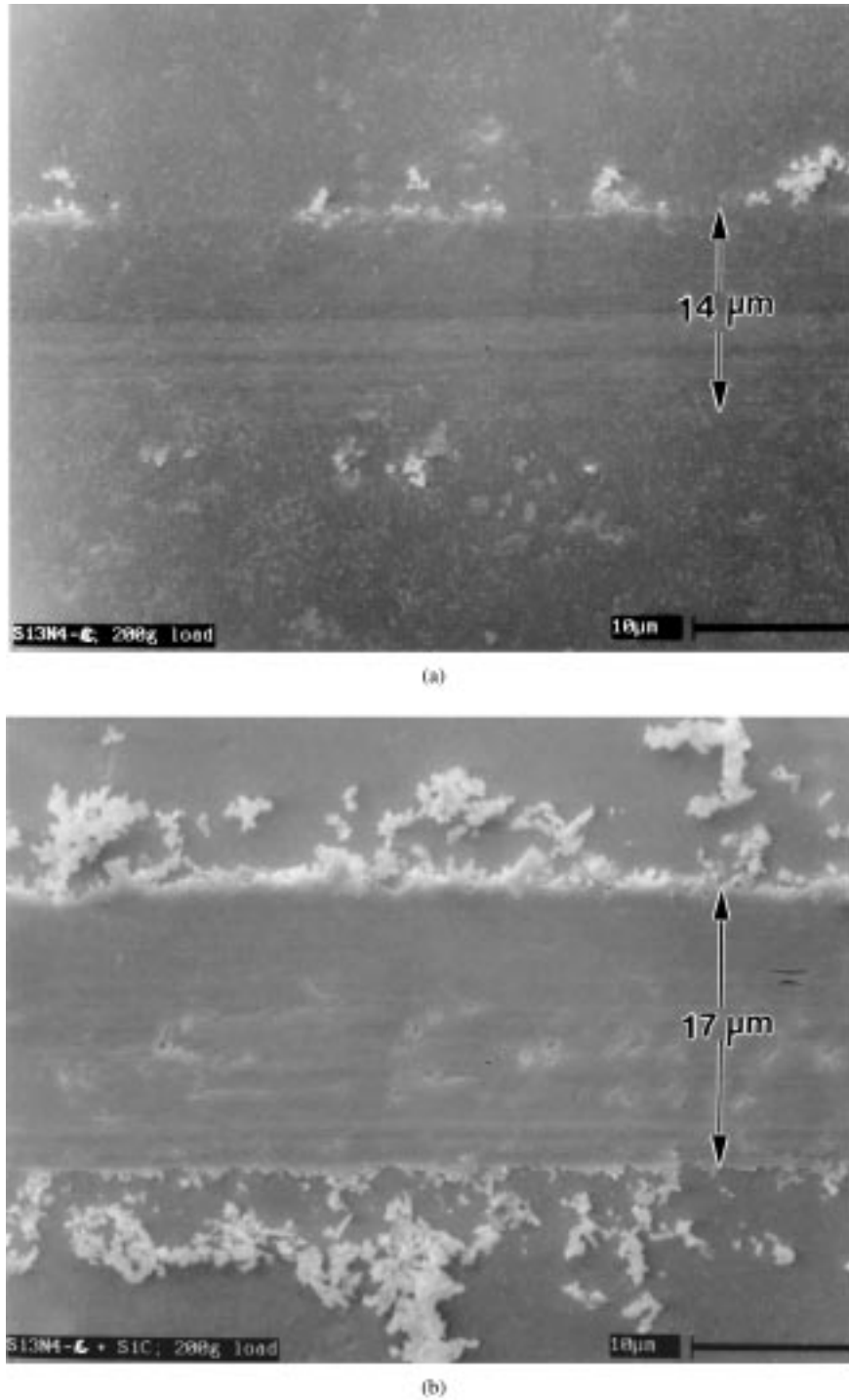

Figure 3 Secondary electron images of single scratches produced by a 20 μm conical diamond under a normal load of 200 grams and a constant speed of 100 μm/min (scratch widths are indicated). (a) Si_3N_4-C; (b) Si_3N_4-C + SiC_w; (c) 99.8%Al_2O_3; and (d) Al_2O_3 + SiC_w. (*Continued*)

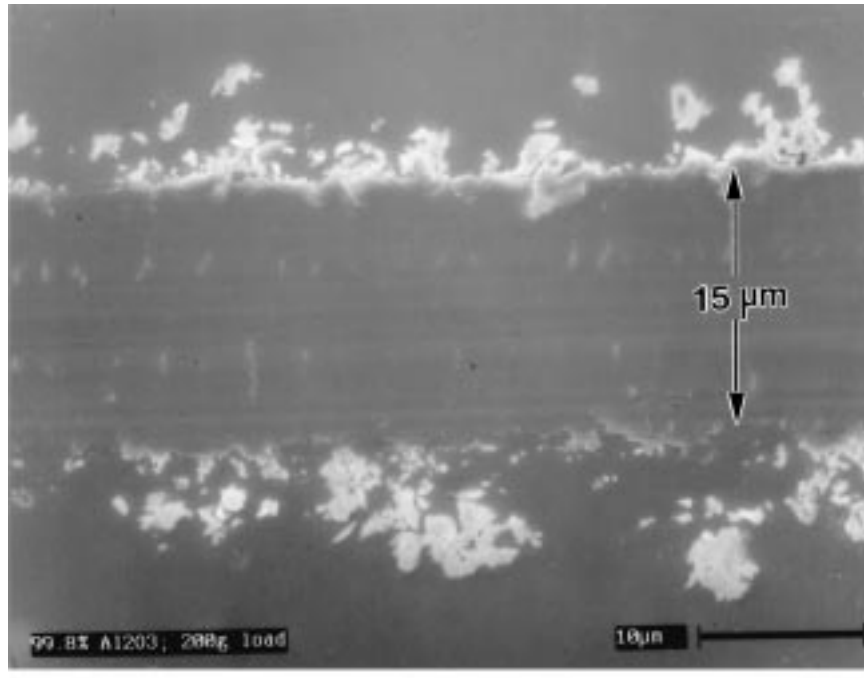

(c)

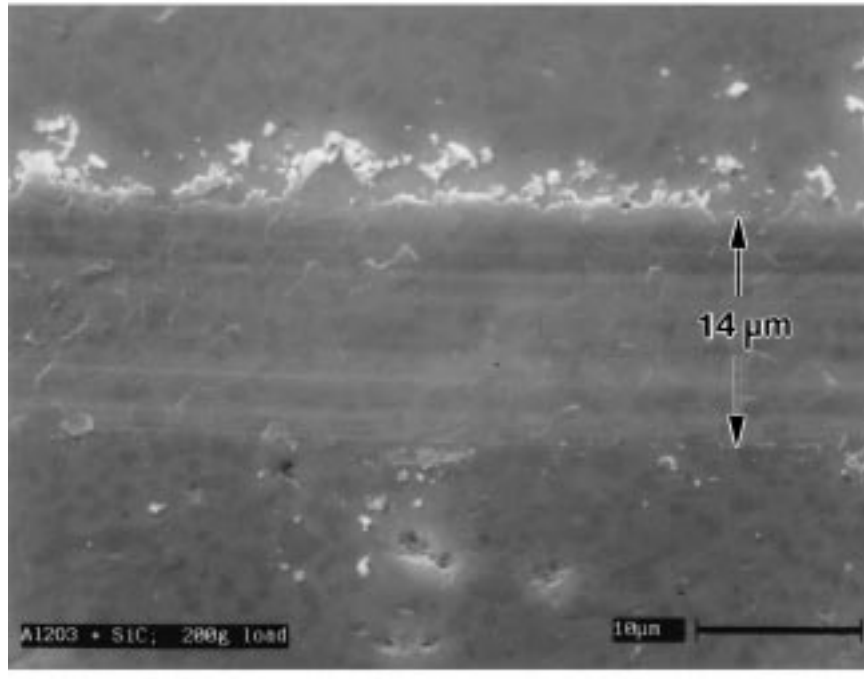

(d)

Figure 3 (*Continued*).

(Fig. 4a and b) is wear sheet formation and plastic grooving, although fracture at wear groove peripheries and delamination within the grooves is also readily apparent. Because of the relatively lower hardness of Si_3N_4-C, the SiC abrasive particles can penetrate more deeply into the surface of the monolith than into that of the composite, leaving deeper scratches in the wear surface of the monolithic material. However, in spite of the higher hardness and toughness of the Si_3N_4-C + SiC_w composite, there are no obvious differences in the wear mechanisms in the two materials. In fact, the wear surface of the composite (Fig. 4b) shows more evidence of fracture, consistent with its higher measured wear rate.

For the glass bonded silicon nitride materials, wear sheet formation and plastic grooving are again the primary responses to the 100 μm SiC wear environment, although the relatively lower hardness of the Si_3N_4-G series results in deeper penetration by the abrasive particles, and therefore, a thicker wear sheet. Although delamination fracture is not as obvious within the wear grooves created in these materials, subsurface fracture at the groove peripheries is more extensive, leading to relatively more material removal than in the series C silicon nitrides. In both Si_3N_4-C + SiC_w and Si_3N_4-G + SiC_w, evidence of whisker debonding and removal is apparent within the fractured regions.

In the alumina-based ceramics worn against the 100 μm SiC (Fig. 4c and d), plastic deformation plays much less of a role in the materials' response to the wear environment. Because of their relatively high

hardness, the wear sheets produced at the surfaces of 99.8%Al_2O_3 and the alumina composite are relatively thin, and the grooves created by the abrasive particles are correspondingly shallow. Delamination fracture of the wear sheet extends into the bulk of the material, resulting in subsurface material removal. The mode of subsurface fracture in both ceramics is almost entirely intergranular.

Wear against the 58 μm SiC abrasive results in the activation of similar types of damage mechanisms in all of the ceramics examined, although the degree of damage and material removal is less severe. Against the 37 μm SiC and 100 μm Al_2O_3 abrasives, however, damage transitions to the mild wear regime and is expressed primarily by the formation of a wear sheet, with only shallow scratches formed by individual abrasive particles. Fracture, which initiates primarily at microstructural heterogeneities, is minimal in these wear surfaces, although more obvious in the composites than in the monolithic materials.

4. Discussion

It is clear from the results of this study that a simple increase in the bulk hardness and/or toughness of a ceramic-based material, through the addition of randomly oriented whisker reinforcement, does not always translate into improved performance in an abrasive

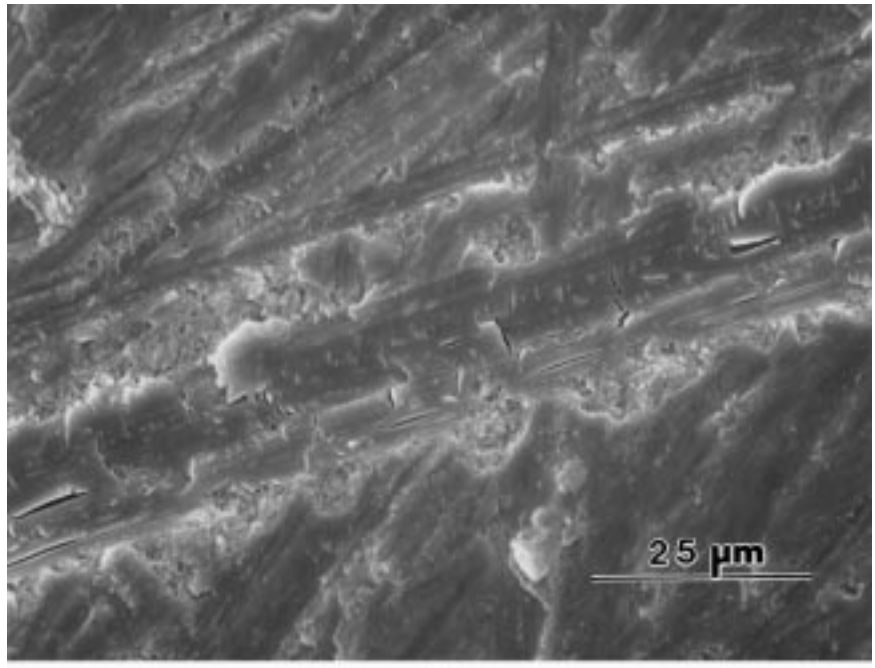

Figure 4 Secondary electron images of the wear surfaces following abrasion against 100 μm (150-grit) SiC particles. (a) Si_3N_4-C; (b) Si_3N_4-C + SiC_w; (c) 99.8%Al_2O_3; and (d) Al_2O_3 + SiC_w. (*Continued*)

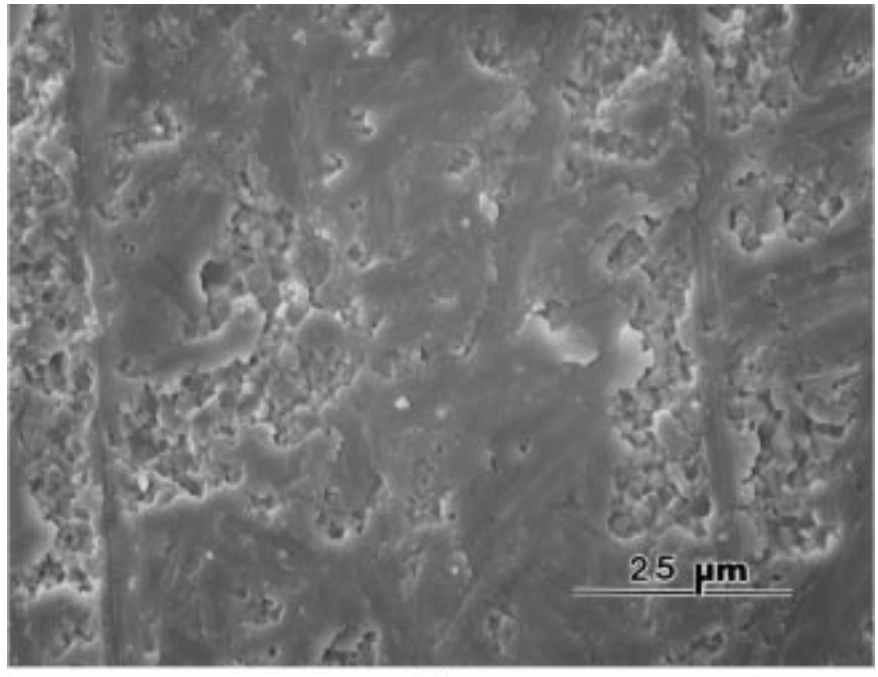

(c)

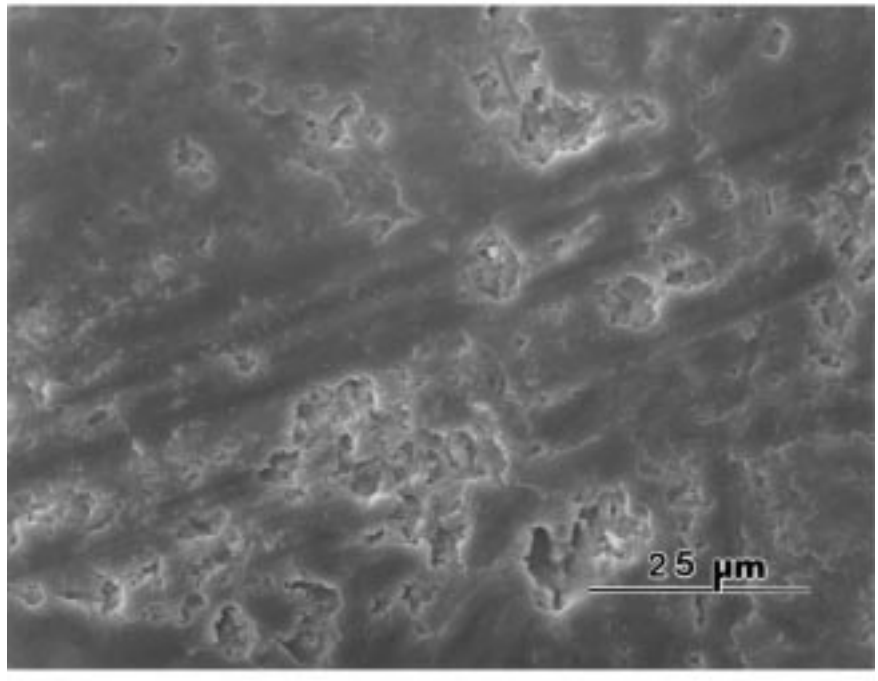

(d)

Figure 4 (*continued*).

wear environment. For example, the addition of 15 volume percent silicon carbide whiskers to the Si_3N_4-C matrix results in a 22% increase in the hardness of the material and a 20% increase in the fracture toughness. Yet, for the most part, the abrasive wear behavior is either unchanged or degraded by the presence of these whiskers. On the other hand, the addition of SiC whiskers to a high-Al_2O_3 matrix, results in a 23% increase in the hardness and a 35% increase in the fracture toughness in comparison to a 99.8%Al_2O_3. And in this case, the addition of SiC whiskers provides a dramatic improvement in the abrasive wear resistance of the ceramic. One possible explanation for this variation in the effect of whisker reinforcement on the wear behavior of ceramic-based composites may reside in the microstructures of these materials, and in the residual stresses created by the addition of second phases to the ceramic. A second important aspect is the influence that the variables of the wear environment have on the wear behavior of the composite.

4.1. Influence of microstructure

Variations in the microstructures of the monolithic materials, as well as in the microstructures of the composites, can often be linked to variations in the abrasive wear behavior through their role in the creation of internal stress. In ceramics it is well known that differences in the thermal expansion between phases of a multiphase material, as well as anisotropic thermal

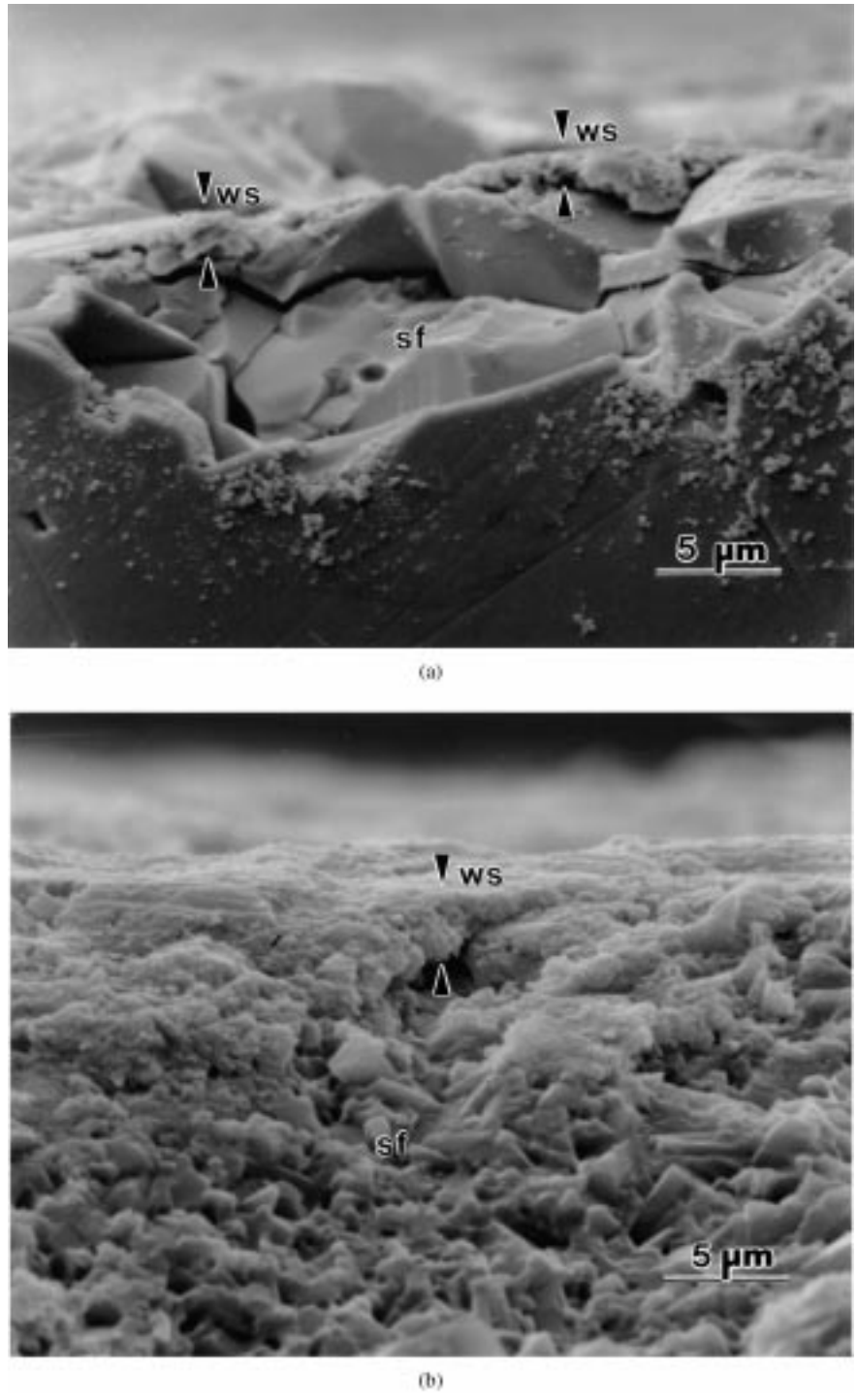

Figure 5 Secondary electron images of a cross section of the pin-on-drum wear surface following abrasion against a 150-grit SiC cloth. (a) A high-alumina ceramic and (b) Si_3N_4-G. In these micrographs, "ws" refers to wear sheet and "sf" refers to subsurface fracture.

expansion in a single phase material, can result in the creation of residual tensile and compressive stresses at hetero- and homophase boundaries. Such residual stresses have been predicted and measured in materials similar to those of this study [4, 41–45]. The magnitude of these local stresses, which are proportional to both the expansion mismatch ($\Delta\alpha$) and the temperature range over which the stresses develop (ΔT), can be sufficient to directly influence the tribological performance of the bulk ceramic [21–23, 46–50]. In the unreinforced silicon nitrides of this study, a difference in the grain boundary microstructures leads to a difference in the local stress state at the grain boundaries of the two materials, and therefore, to a difference in abrasive wear behavior. In Si_3N_4-C, the grain boundary regions have almost completely crystallized to $Y_2Si_3N_4O_3$ and β-$Y_2Si_2O_7$, whereas in Si_3N_4-G the grain boundary regions consist of an amorphous yttrium aluminosilicate phase. Although the thermal expansion coefficients of the boundary phases have not been measured, it is expected that crystalline $Y_2Si_3N_4O_3$, a member of the gehlenite family, has a coefficient of thermal expansion in the range of $1–2 \times 10^{-6}/^{\circ}C$ over the temperature range of 25° to 1000°C [51]. This is somewhat lower than the coefficient of thermal expansion of β-Si_3N_4 over the same temperature range ($\alpha = 3.0 \times 10^{-6}/^{\circ}C$)

and results in the boundaries in Si_3N_4-C being left in residual compression at room temperature while the matrix grains are in residual tension. (Recall that TEM observations suggest that a residual stress exists at many of the heterophase boundaries in this material.) The net result is an increase in the local fracure toughness of the boundary regions, making them more resistant to fracture in an abrasive environment. In contrast, the amorphous boundary phase present in the Si_3N_4-G is estimated to have a coefficient of thermal expansion of around $5 \times 10^{-6}/^{\circ}C$ [52], which is higher than that of the β-Si_3N_4 matrix, and which therefore leaves the boundaries in residual tension. Such a residual stress state would be expected to decrease the local fracture toughness, providing an easier fracture path through the grain boundaries under the stresses imposed by the abrasive environment. As a result of their residual stress states, Si_3N_4-C tends to be more resistant to abrasive wear environment than is Si_3N_4-G. Matrix grain size and grain shape are also known to influence the fracture toughness of silicon nitride ceramics [6], and therefore the wear resistance, and these effects are no doubt combined with those created by the thermal expansion mismatch in these ceramics. While the matrix grain shape is essentially the same in both silicon nitrides, the average matrix grain size of Si_3N_4-G is approximately twice that of Si_3N_4-C.

The addition of SiC whiskers to these matrices results in an increase in the hardness of the composites and, in the case of Si_3N_4-C, an increase in bulk fracture toughness. But, the glass phase which wests the SiC whiskers in both Si_3N_4-based composites creates a relatively weak interface that leads to easy debonding of the whisker during fracture-type events (the origin of enhanced long-crack fracture toughness). As a result of this debonding, the SiC whiskers are easily pulled from the surface of the composites in an abrasive wear environment, leading to increased material removal, and degradation of the wear properties when compared to the monolithic Si_3N_4. Regions of whisker debonding are apparent at the wear surfaces of both Si_3N_4-based composite materials. This effect is also apparent in the results of the single scratch tests, and particularly for the Si_3N_4-C materials, where there is far more fracture associated with a given scratch in the composite material than there is for an identical scratch in the monolithic ceramic (compare for example Fig. 3a and b).

In the alumina-based ceramics, a similar effect of microstructure on tribological properties is observed. Matrix grain size plays a decisive role in determining the abrasive wear behavior in many alumina ceramics [21–23, 46–50], with wear resistance generally increasing with decreasing grain size according to a Hall-Petch type relationship. Enhancing the grain size effect is the influence of grain boundary phases on the residual stress state of the alumina ceramics [21, 22]. The two aluminas of this study have very different boundary microstructures: the 99.8% Al_2O_3 contains graphite at many boundaries, whereas the composite is glass-bonded, with an amorphous magnesium aluminosilicate boundary phase. Nonetheless, both graphite and the Mg-aluminosilicate glass are expected to have average coefficients of thermal expansion between 4 and $5 \times 10^{-6}/^{\circ}C$, which puts their boundaries in residual compression and thus increases the local fracture toughness. The combination of small matrix grain size and locally tough grain boundaries makes the 99.8%Al_2O_3 a more wear resistant material than many other high-alumina ceramics tested under identical wear conditions [39]. In the composite material, the addition of the relatively lower expansion SiC whiskers to the glass-bonded alumina matrix sets up residual compressive stresses at the whisker-matrix and whisker-glass interfaces. As a result, the whisker-matrix interfaces are again locally tougher, resisting the debonding and pull-out of the SiC whiskers in the abrasive wear environment under all test conditions of this study. Thus retained, the SiC whiskers, with their higher hardness, are available at the surface to enhance the wear resistance of the composite material. Under all conditions of this study, the alumina-based composite is between 80% and 250% more wear resistant than the 99.8% Al_2O_3, in spite of its larger matrix grain size.

4.2. Influence of the wear environment

Variables in the wear environment combine with variables in the material properties (and microstructure) to determine the wear resistance of a composite material. Under the relatively "softer" abrasive wear conditions of the alumina abrasive, the primary response of all composites is plastic deformation with only limited fracture. However, the presence of whisker reinforcement in the silicon nitrides tends to increase the amount of fracture observed at the wear surface relative to that of the monolithic materials. This results in a higher measured wear rate and suggests that the relatively weaker Si_3N_4–SiC interfaces are the origin of this increased surface fracture. Under the more aggressive conditions of the harder SiC abrasive, SiC whisker debonding and pullout in the Si_3N_4 composites results in a higher wear rate, as described in the previous section. Because of the stronger matrix-whisker interfaces in the $Al_2O_3 + SiC_w$ composite, this material performs well under both "soft" and "hard" abrasive conditions.

While abrasive particle size does influence the measured wear rate of both the monolithic ceramics and the ceramic composites (increasing the abrasive wear rate with increasing particle size, see Fig. 2), it is only when the abrasive particle size is small that the composite becomes more wear resistant than the matrix material. In this study, this phenomenon is observed for the Si_3N_4-C materials in wear tests against 37 μm SiC, where the composite is 25% more wear resistant than the monolithic material. In this case, such a change in the relative ranking of composite and monolithic materials is more likely due to the stress state created by the wear environment than to any differences in the microstructure between the two materials. SEM analyses of the various abrasive cloths used in this study indicate that while abrasive particle size does scale, as expected, with grit size, the average particle shape does not, and more importantly, the average contact area per abrasive particle does not change greatly with grit size. However, because the number of contact points per unit area increases with decrease in abrasive particle size, there are

approximately a factor of 10 more load-carrying points per unit area for a 400-grit cloth than for a 150-grit abrasive cloth [53]. Thus, the average load per abrasive particle is reduced, and the wear rate is correspondingly lower at smaller abrasive particle sizes. For the Si_3N_4-C composite, the stresses created by the 400-grit (37 μm) SiC particles under the conditions of this study are no longer sufficient to cause significant penetration of the wear surface or large-scale debonding and fracture of the whisker reinforcement, and the wear rate is correspondingly reduced. Because the hardness and toughness of the Si_3N_4-G composite are lower, a similar effect is not observed in that material over the range of abrasive sizes used in this study.

5. Conclusions

Study of the influence of randomly-oriented SiC whisker reinforcement on the abrasive wear behavior of silicon nitride- and alumina-based ceramics indicates that simple increases in bulk hardness and fracture toughness through the addition of whisker reinforcement will not always lead to enhanced wear resistance. Instead the results of this study suggest attention should focus on the residual stress state of the whisker-matrix interface in whisker-reinforced composites, and its influence on the local fracture toughness, in order to understand abrasive wear behavior. The addition of SiC whiskers to a Si_3N_4 matrix sets up tensile stresses at the whisker-matrix interfaces, enhancing the bulk toughness of the composite, but degrading the abrasive wear properties by promoting easier whisker debonding and removal by the abrasive particles. The addition of SiC whiskers to an alumina matrix, on the other hand, results in the creation of compressive stresses at the whisker-matrix interface, producing a relatively stronger bond that can better withstand the rigors of an abrasive wear environment. As a result, the $Al_2O_3 + SiC_w$ composite is consistently a more wear resistant material than are the $Si_3N_4 + SiC_w$ composites.

A similar effect of microstructure is noted in the unreinforced materials. In the case where grain boundaries are left in residual compression at room temperature, the local fracture toughness of these regions is increased, enhancing the material's wear resistance in an abrasive environment. Boundaries which are left in residual tension are more susceptible to fracture, and result in more material removal in the wear environment. In many cases, these changes in local toughness are not reflected in a bulk toughness measurement.

These results imply that a compromise may be necessary in the design of materials that are expected to be macrostructurally tough and yet withstand the rigors of an environment where fracture events on a microstructural scale are also important.

Acknowledgments

The authors would like to thank Ms. Henrietta Clancy, formerly with the Albany Research Center, and Mr. Dale Govier of the Albany Research Center for their help with the metallography and the X-ray diffraction analyses used in this study.

References

1. M. RÜHLE, B. J. DALGLEISH and A. G. EVANS, *Scripta Metall.* **21** (1987) 681.
2. P. F. BECHER, C.-H. HSEUH, P. ANGELINI and T. N. TIEGS, *J. Am. Ceram. Soc.* **71** (1988) 1050.
3. P. G. CHARALAMBIDES and A. G. EVANS, *ibid.* **72** (1989) 746.
4. G. H. CAMPBELL, M. RÜHLE, B. J. DALGLEISH and A. G. EVANS, *ibid.* **73** (1990) 521.
5. M. BENGISU, O. T. INAL and O. TOSYALI, *Acta Metall. Mater.* **39** (1991) 2509.
6. P. F. BECHER, *J. Am. Ceram. Soc.* **74** (1991) 255.
7. P. ŠAJGALIK, J. DUSZA and M. J. HOFFMAN, *ibid.* **78** (1995) 2619.
8. J. A. HAWK and C. P. DOĞAN, in "Advanced Ceramics for Structural and Tribological Applications," edited by H. M. Hawthorne and T. Troczynski (CIM, Montreal, Quebec, Canada, 1995) p. 139.
9. T. YAMAMOTO, M. OLSSON and S. HOGMARK, *Wear* **174** (1994) 21.
10. C. S. YUST, J. M. LEITNAKER and C. E. DEVORE, *ibid.* **122** (1988) 151.
11. S. C. FARMER, C. DELLACORTE and P. O. BOOK, *J. Mater. Sci.* **28** (1993) 1147.
12. H. LIU, M. E. FINE and H. S. CHENG, *J. Am. Ceram. Soc.* **74** (1991) 2224.
13. D. WANG and Z. MAO, *ibid.* **78** (1995) 2705.
14. S. W. LEE, S. M. HSU and R. G. MUNRO, in "Tribology of Composite Materials," edited by P. K. Rohatgi, P. J. Blau, and C. S. Yust (ASM, Metals Park, OH, 1990) p. 35.
15. M. BOHMER and E. A. ALMOND, *Mat. Sci. Eng. A* **105/106** (1988) 105.
16. J. R. GOMES, M. I. OSENDI, P. MIRANZO, F. J. OLIVEIRA and R. F. SILVA, *Wear* **233–235** (1999) 222.
17. V. S. R. MURTHY, K. SRIKANTH and C. B. RAJU, *ibid.* **223** (1998) 79.
18. M. A. MOORE and F. S. KING, *ibid.* **60** (1980) 123.
19. A. G. EVANS and D. B. MARSHALL, in "Fundamentals of Friction and Wear of Materials," edited by D. A. Rigney (ASM, Metals Park, OH, 1980) p. 439.
20. T. A. LIBSCH, P. C. BECKER and S. K. RHEE, *Wear* **111** (1986) 263.
21. C. P. DOĞAN and J. A. HAWK, *ibid.* **181–183** (1995) 129.
22. C. P. DOĞAN and J. A. HAWK, in "Advanced Ceramics for Structural and Tribological Applications," edited by H. M. Hawthorne and T. Troczynski (CIM, Montreal, Quebec, Canada, 1995) p. 181.
23. S.-J. CHO, B. J. HOCKEY, B. R. LAWN and S. J. BENNSION, *J. Am. Ceram. Soc.* **72** (1989) 1249.
24. S. M. HSU, V. S. NAGARAJAN and H. LIU, in "Advanced Ceramics for Structural and tribological Applications," edited by H. M. Hawthorne and T. Troczynski (CIM, Montreal, Quebec, Canada, 1995) p. 7.
25. G. R. ANSTIS, P. CHANTIKUL, B. R. LAWN and D. B. MARSHALL, *J. Am. Ceram. Soc.* **64** (1981) 533.
26. R. BLICKENSDERFER and G. LAIRD, II, *J. Test. Eval.* **16** (1988) 516.
27. DIN 50 321, Verschleiss-Messgroessen (Beuth Verlag, Berlin, 1979).
28. "1992 Annual Book of ASTM Standards, Vol. 03.02: Wear and Erosion; Metal Corrosion" (ASTM, Philadelphia, PA, 1992) p. 248.
29. M. WILKENS and M. RÜHLE, *Phys. Status Solidi B* **49** (1972) 749.
30. I. H. HUTCHINGS, in "Advanced Ceramics for Structural and Tribological Applications," edited by H. M. Hawthorne and T. Troczynski (CIM, Montreal, Quebec, Canada, 1995) p. 127.
31. J. LARSEN-BASSE and B. PREMARATNE, in " Wear of Materials," edited by K. C. Ludema (ASME, New York, NY, 1982) p. 161.
32. B. R. LAWN, N. P. PADTURE, H. CAI and F. GUIBERTEAU, *Science* **263** (1994) 1114.
33. Z. BI, H. TOKURA and M. YOSHIKAWA, *J. Mat. Sci.* **23** (1988) 3214.
34. H. P. KIRCHNER and E. D. ISSACSON, *J. Am. Cream. Soc.* **65** (1982) 55.

35. C. P. DOĞAN and J. A. HAWK, "Abrasive Wear of Silicon Nitride Based Materials," in preparation.
36. C. P. DOĞAN and J. A. HAWK, *Wear* **212** (1997) 110.
37. *Idem.*, "Influence of Microstructure on the Abrasive Wear Behavior of Structural Ceramics," in preparation.
38. B. J. HOCKEY, *J. Am. Ceram. Soc.* **54** (1971) 223.
39. C. P. DOĞAN and J. A. HAWK, *Wear* **225–229** (1999) 1050.
40. M. ODÉN and T. ERICSSON, *J. Am. Ceram. Soc.* **79** (1996) 2134.
41. C. A. POWELL-DOĞAN and A. H. HEUER, *ibid.* **73** (1990) 3684.
42. Q. MA and D. R. CLARKE, *ibid.* **77** (1994) 298.
43. I. M. PETERSON and T.-Y. TIEN, *ibid.* **78** (1995) 2345.
44. R. H. DAUSKARDT and J. W. AGER III, *Acta Mater.* **44** (1996) 625.
45. P. E. BECHER, E. Y. SUN, C.-H. HSUEH, K. B. ALEXANDER, S.-L. HWANG, S. B. WATERS and C. G. WESTMORELAND, *ibid.* **44** (1996) 3881.
46. C. CM. WU, R. W. RICE, D. JOHNSON and B. A. PLATT, *Ceramic Eng. Sci. Proc.* **6** (1985) 995.
47. H. H. K. XU, S. JAHANMIR and Y. YANG, *J. Am. Ceram. Soc.* **78** (1995) 881.
48. C. HE, Y. S. WANG, J. S. WALLACE and S. M. HSU, *Wear* **162–164** (1993) 314.
49. O. O. AJAYI and K. C. LUDEMA, in "Wear of Materials, Vol. I," edited by K. C. Ludema and R. G. Bayer (ASME, New York, NY, 1991) p. 307.
50. R. M. ANDERSON, T. A. ADLER and J. A. HAWK, *Wear* **162–164** (1993) 1073.
51. P. G. ORSINI, A. BURI and A. MAROTTA, *J. Am. Ceram. Soc.* **58** (1975) 306.
52. W. E. S. TURNER, *ibid.* **12** (1929) 760.
53. H. SIN, N. SAKA and N. P. SUH, *Wear* **55** (1979) 163.

Received 1 March
and accepted 8 May 2000